

# Analysis of Skylab II S193 Scatterometer Data

ARTHUR K. JORDAN, CHARLES G. PURVES, AND JAMES F. DIGGS

*Aerospace Systems Branch  
Space Systems Division*

May 2, 1975



**NAVAL RESEARCH LABORATORY**  
Washington, D.C.

Approved for public release; distribution unlimited.



In the absence of a large body of Ku-band ocean radar data, the results of the NRL experiments at X-band (8.9 GHz) were used for comparison. The S193 data of June 5, 1973, when a practically uniform wind field was present, show reasonable agreement with the NRL empirical and theoretical models. The data of June 6, 1973, are more complex, due to rapid variations in wind speeds and directions around Hurricane AVA. The NRL empirical model was interpolated to account for variation in wind heading relative to the S193 antenna pointing direction; a reasonable comparison could then be made with the corresponding S193 data of June 6, 1973. More scatterometer data should be analyzed in order to obtain correlations between variations in ocean parameters and radar cross section measurements.

**CONTENTS**

INTRODUCTION. . . . .	1
DATA ANALYSIS. . . . .	2
CONCLUSIONS AND RECOMMENDATIONS . . . . .	13
ACKNOWLEDGEMENTS . . . . .	13
REFERENCES. . . . .	14

## ANALYSIS OF SKYLAB II S193 SCATTEROMETER DATA

## INTRODUCTION

Global measurements of ocean winds can provide useful information for the prediction of weather and sea conditions. The SEASAT System [1,2] has been proposed to acquire data for large portions of the ocean surface. As presently planned, SEASAT will incorporate an altimeter, an imaging radar, and a scatterometer. By measuring the radar cross section from the ocean, the scatterometer will be able to supply information about ocean capillary waves and, possibly, local surface winds. Several programs, notably SKYLAB [3], have provided preliminary measurements that are relevant to the design and the mission of the proposed SEASAT system.

The Naval Research Laboratory has a continuing program for the measurement and analysis of radar scattering from the oceans. The mechanisms for sea scattering have been investigated in great detail, and voluminous ocean scattering data have been collected, analyzed, and related to wind conditions [4,5,6,7]. In particular, the NRL Four-Frequency Radar (4FR) System has been used in an airplane to obtain microwave scattering data from oceans in various parts of the Earth [8,9]. It would be advantageous to extend the domain of ocean radar data to include the synoptic measurements that are being provided by radars on board orbiting Earth satellites.

The SKYLAB S193 radiometer/scatterometer/altimeter experiment provided oceanographers and meteorologists with the means of simultaneously measuring the backscattering cross section and the thermal radiation of the land and ocean on a global scale. The active radar scatterometer and the passive radiometer operated at the same frequency, 13.9 GHz (Ku-band). The scatterometer measured the normalized backscattering cross section,  $\sigma^{\circ}(\theta)$ , as a function of incidence angle,  $\theta$ , and polarization, VV, VH, HH, or HV. The radiometer measured the apparent brightness temperature,  $T(\theta)$ , from an observed area on the Earth's surface. All data were recorded on magnetic tape on one digitized channel.

The "sea truth", i.e., the ocean wind and weather conditions obtained by instruments on low-flying aircraft and surface vessels, was correlated with the corresponding S193 measurements made on several SKYLAB passes [10]. Then the measured radar cross sections of the ocean were compared with predictions made using established theoretical [5,7] and empirical [9] models.

A pilot program was undertaken to make an independent comparison of the SKYLAB S193 scatterometer data with the extensive NRL measurements of radar scattering from the ocean. The purpose of this program was to aid in the evaluation of the S193 data for future applications. An analysis of the scatterometer data for the passes of June 5, 1973, over the Gulf of Mexico and June 6, 1973, over Pacific Hurricane AVA has been

---

Note: Manuscript submitted February 20, 1975.

made. This report summarizes the analysis, which was carried out at NRL to determine the validity of the SKYLAB II S193 data and their applicability for oceanographic research.

## DATA ANALYSIS

The tabulated data for the SKYLAB passes on June 5 and 6, 1973, [11,12] were used in this analysis. The instrumentation and data processing for the S193 experiment have been described previously [3,13].

The computed fields of view (FOV's) [11,12] were plotted for five scan angles, as shown in Figs. 1 and 2. The actual angles of incidence,  $\theta$ , differed slightly from these values due to the effects of the Earth's curvature and the changing attitudes of SKYLAB. Figure 1 shows the FOV positions for the two extreme scan angles, and Fig. 2 shows the positions for all five angles. On June 5, the S193 was used in the in-track noncontiguous (ITNC) mode to acquire data (Fig. 1) with overlapping measurements along the subsatellite track. The scan angles between the antenna pointing direction and the vertical at the spacecraft were  $0^\circ$ ,  $15^\circ$ ,  $29^\circ$ ,  $40^\circ$ , and  $48^\circ$ . On June 6, the S193 was used in the cross-track noncontiguous (CTNC) mode to acquire data (Fig. 2) with nonoverlapping measurements perpendicular to the subsatellite track and with the same scan angles. The footprints for the different scan angles are given in Fig. 3a; the measurement times for the scatterometer for each angle are given in Fig. 3b. The measured  $\sigma^\circ(\theta)$  were calculated from the integrated powers; thus, the tabulated values of  $\sigma^\circ(\theta)$  [11,12] are the mean values averaged over the integration times for each mode [13, p. 2-216; 1, Table 2.1-2].

The tabulated values of  $\sigma_{\text{HH}}^\circ(\theta)$  are plotted as functions of time in Fig. 4, and the values of  $\sigma_{\text{VV}}^\circ(\theta)$  are plotted in Fig. 5; the data points shown are for measurements made over the water only on June 5. A practically uniform wind field was present over the FOV's of the June 5 pass, as shown by both the synoptic weather data and observations made on the C-130 underflight [10]. Averaging over a time period was possible for these data, and the standard deviations were relatively small, as shown in Table 1. It is interesting to note that the FOV indicated by the asterisk in Fig. 1 is located over shallow water (the Granville Shoal just north of the Yucatan Peninsula). The corresponding values of  $\sigma^\circ$ , indicated by asterisks in Figs. 4 and 5, are much lower than the corresponding values for FOV's over deep water. Possibly the presence of natural slicks, seaweed, and calm, shallow water caused the decrease in reflected power. This data point was not included in the averages given in Table 1.

In the absence of a large body of applicable Ku-band (13.9 GHz) data, the normalized cross sections,  $\sigma_{\text{VV}}^\circ(\theta)$ , were calculated using the NRL empirical model [9] for X-band (8.9 GHz) data with wind speeds measured on the C-130 underflights (in this case,  $\sim 13$  knots). As shown in Fig. 6 for  $\sigma_{\text{VV}}^\circ(\theta)$  data of June 5, the relationship between the NRL X-band data and the averaged SKYLAB data points given in Table 1 is practically constant. The differences between the two sets of data can be ascribed to the frequency difference of 5.0 GHz.

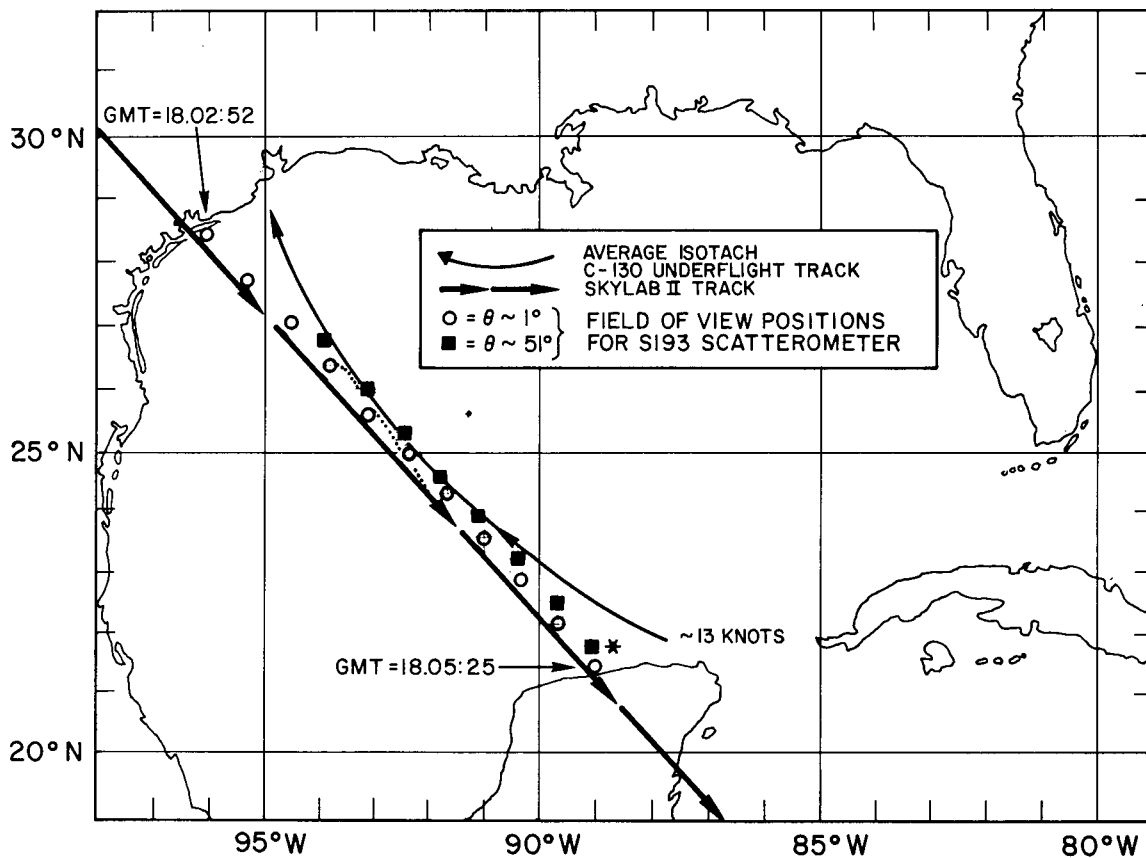


Fig. 1 — Field of view positions (ITNC Mode) of the S193 scatterometer, VV polarization, for the SKYLAB II pass of June 5, 1973, with an average isotach correlated to the sea truth.

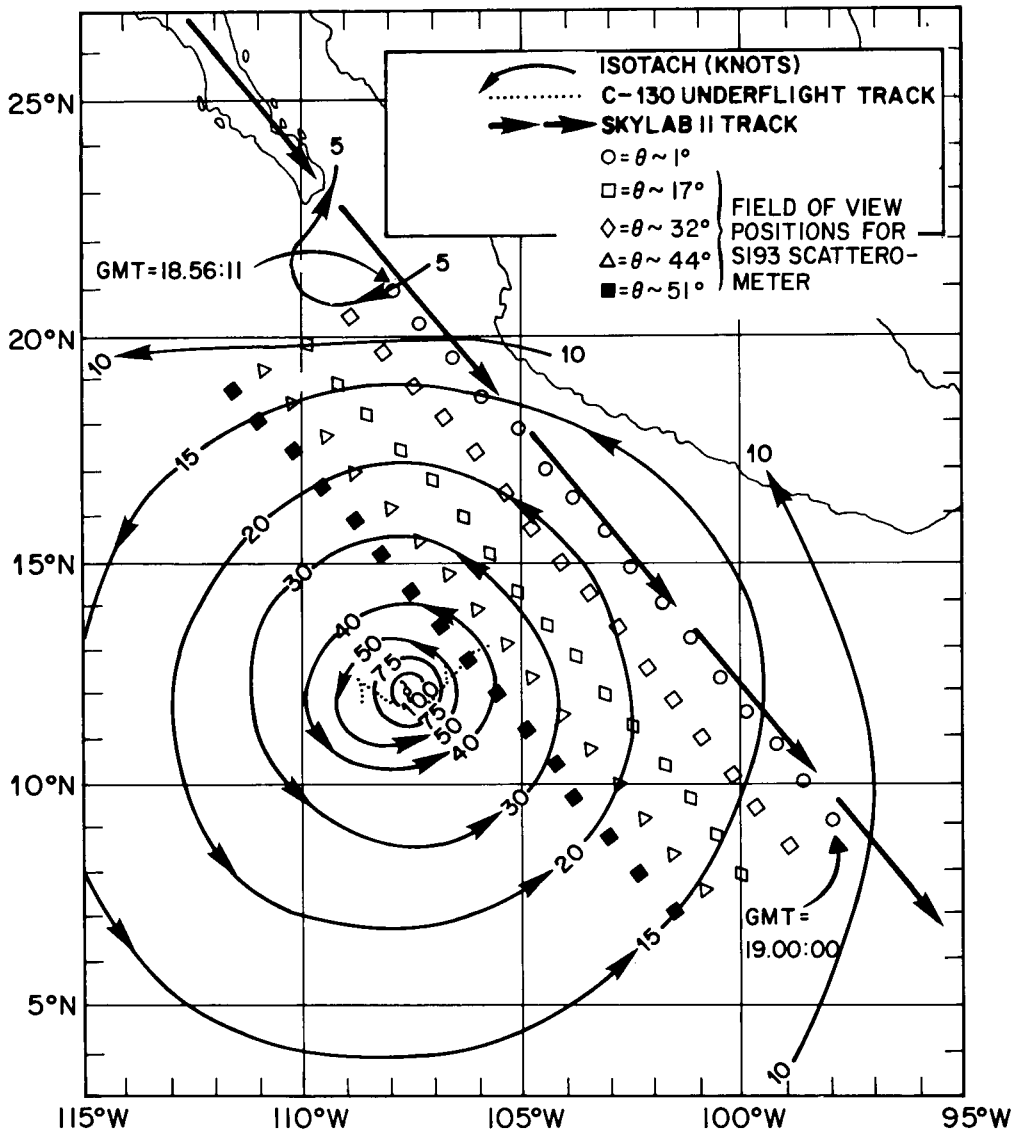


Fig. 2 -- Field of view positions (CTNC Mode) of the S193 scatterometer, VV polarization, for the SKYLAB II pass of June 6, 1973, with isotach analysis.

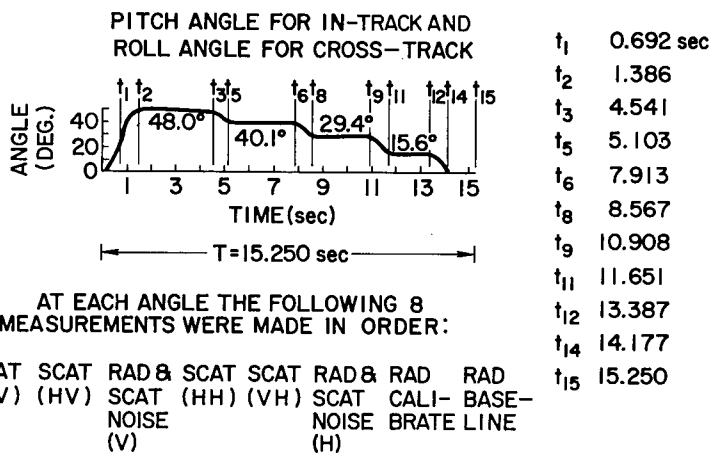
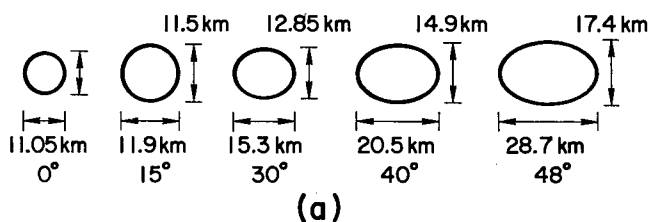


Fig. 3 — (a) Footprint outlines for ITNC and CTNC modes. (b) Timing and scan angles for S193 radiometer/scatterometer, CTNC and ITNC modes ([1], Fig. 1.3.3).

JORDAN, PURVES, AND DIGGS

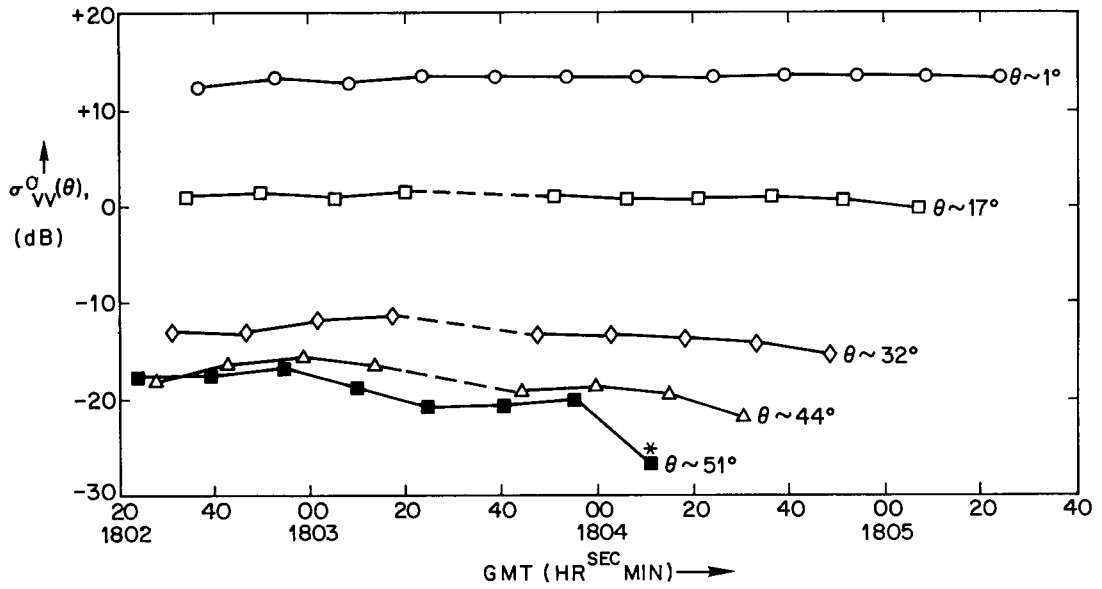


Fig. 4 — Normalized cross-section  $\sigma_{VV}^o(\theta)$ , as a function of time from S193 data for June 5, 1973 (missing data points are interpolated with dashed line).

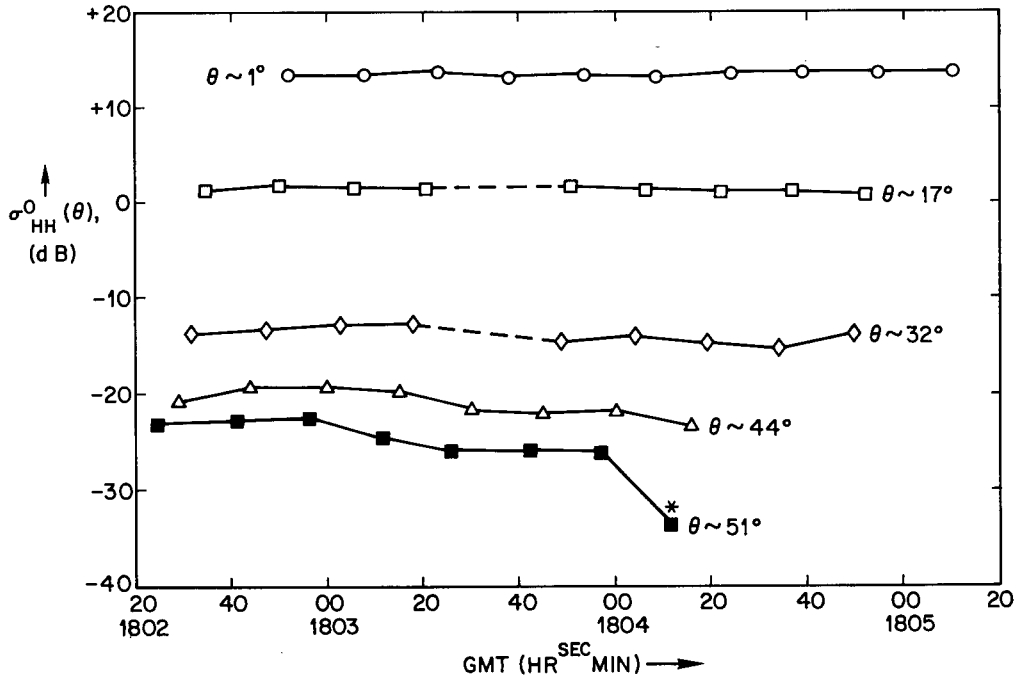


Fig. 5 — Normalized cross-section  $\sigma_{HH}^o(\theta)$ , as a function of time from S193 data for June 5, 1973 (missing data points are interpolated with dashed line).

Table 1  
 SKYLAB II, June 5, 1973, Pass 5  
 (Averages of Over-Water Points Used in Figure 6)

Start Time			End Time			Number Of Data Points	Averages		Standard Deviations	
Hr	Min	Sec	Hr	Min	Sec		$\bar{\theta}$ , (degrees)	$\bar{\sigma}_{VV}^{\circ}$ , (dB)	$\theta$ , (degrees)	$\sigma_{VV}^{\circ}$ , (dB)
18	02	24.2	18	04	10.9	7	50.44	-18.84	0.14	1.71
18	02	27.8	18	04	29.8	8	43.77	-18.23	0.10	2.03
18	02	31.3	18	04	48.5	9	32.09	-13.27	0.08	1.13
18	02	34.3	18	05	6.8	10	16.99	+0.84	0.07	0.45
18	02	52.0	18	05	39.7	11	0.94	+13.39	0.06	0.22

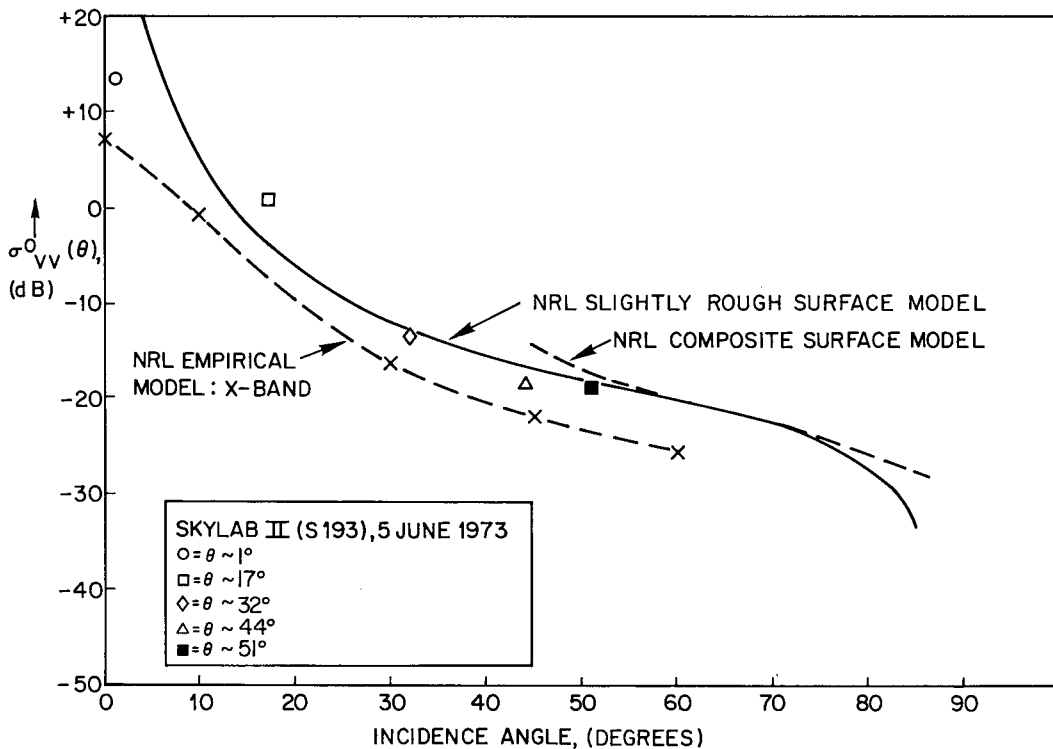


Fig. 6 — Comparison of S193 data, June 5, 1973,  $\sigma_{VV}^{\circ}(\theta)$ , with NRL empirical, composite surface and slightly rough surface models.

The NRL composite surface model [4,5] and slightly rough surface model [7] were used to make theoretical predictions for  $\sigma_{VV}^{\circ}(\theta)$  at 13.9 GHz. Theoretical predictions based on these models have been used successfully in interpreting airborne radar measurements of sea scatter for different wind conditions. Within the limits of validity of the theory, the NRL slightly rough surface model gave good agreement with S193 data (Table 1) that were taken when a relatively uniform wind field was present, as shown in Fig. 6. For the composite surface model to be useful, some estimate must be made of the rms slope of the sea. A correlation between rms slope and wind speed has been made on the basis of a Gaussian slope distribution [5,14]. When this correlation was used, the composite surface model gave reasonable agreement with the SKYLAB measurements between  $\theta \approx 50^{\circ}$  and  $\theta \approx 80^{\circ}$ , as shown in Fig. 6. The particular representation of the general composite surface theory which was implemented at NRL was chosen to provide information for near grazing incidence angles. Thus, for the present application with 13-knot winds, valid numerical results are obtained only for  $\theta > 50^{\circ}$ .

Since the data for Hurricane AVA on June 6, 1973, were considerably more complex and averaging over time was not possible, the data were considered on a point-by-point basis. The dwell times, which varied between 1 and 3 seconds for each scan angle (see Fig. 3), were long enough for the scatterometer to observe significantly different ocean conditions. However, the radar returns within each integration time period were integrated to form a single mean value for power, which was then used in calculating  $\sigma^{\circ}(\theta)$  [3]. High peak wave heights and steep wind gradients are associated with the rapidly changing sea surface conditions prevalent in a hurricane. In the case of the data acquired during Hurricane AVA, the integration of backscatter signals had a tendency to smooth the extremes detected within each FOV.

The variation of normalized cross section with wind heading relative to the antenna pointing direction can provide information about directional wave spectra ([3], Fig. 7, and [15]). Hurricane AVA provided an opportunity to observe this variation, although the tabulated data for June 6 provide a variation in wind heading of approximately  $180^{\circ}$ . In order to infer the wind direction at the surface, one must make corrections for frictional effects. Statistical studies [16] permit reasonably good forecasting rules of thumb, which assume that the gradient wind is  $20^{\circ}$  to  $30^{\circ}$  clockwise with respect to the surface wind and has a velocity nearly equal to the wind velocity at the gradient level, i.e., 1000 to 2000 feet above the surface. On this assumption, the surface wind speeds and directions were calculated from the available data [10] (see Table 2).

The data for Hurricane AVA on June 6, 1973, are more complex since both wind speed and direction had significant point-to-point variations. The NRL empirical model provided predictions for the variation of  $\sigma_{VV}^{\circ}(\theta)$  at X-band with wind heading relative to the antenna for the upwind (UW), downwind (DW), and cross wind (CW) directions, as shown in Figs. 7a and 7b. With the aid of the NASA AAFE Radscat measurements [1], the NRL empirical model was interpolated to obtain the variation of  $\sigma_{VV}^{\circ}(\theta)$  as a function of wind heading relative to the antenna pointing direction; the interpolated curves for four wind speeds are shown in Figs. 8a and 8b. The approximate surface wind speed and direction for each of the FOV's for the S193 can be obtained from Fig. 2. The appropriate wind heading angles relative to the antenna pointing direction were

determined from the knowledge of the direction of the SKYLAB II track and the orientation of the antenna in the CTNC mode. These relative angles are given in Table 2 for two incidence angles,  $45^\circ$  and  $30^\circ$ , which correspond to incidence angles used in the NRL empirical model; the FOV's are identified by their time coordinates given in the tabulations in [11] and [12]. The wind speeds and directions of Hurricane AVA, Fig. 2, were correlated with those of the interpolated NRL empirical model, Fig. 8, so that a comparison (allowing for the 5 GHz difference in radar frequencies) could be made; Fig. 9 shows the comparison for  $45^\circ$  and  $30^\circ$  incidence angles. It was assumed that the hurricane was approximately stationary over the time span of the S193 measurements (approximately  $4\frac{1}{2}$  minutes for the data of Fig. 9); therefore, the time coordinate of Fig. 9 can be related to the relative heading coordinate of Fig. 8. There is a reasonable comparison between the two sets of data until GMT  $\approx 18.58:00$ ; after that time the S193 data and the interpolated NRL model are significantly different.

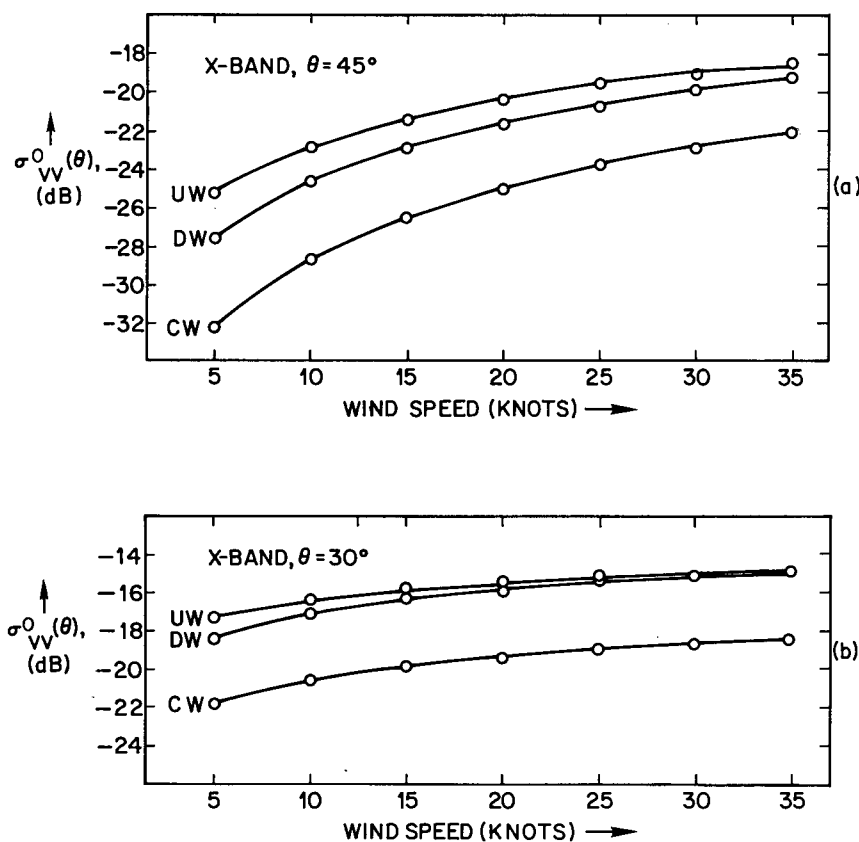


Fig. 7 — Variation of X-Band  $\sigma_{VV}^0(\theta)$  as a function of wind speed for upwind (UW), downwind (DW) and crosswind (CW) cases as determined by NRL empirical model for incidence angles of  $45^\circ$  (a) and  $30^\circ$  (b).

JORDAN, PURVES, AND DIGGS

Table 2  
 Wind Data for Pass AVA, June 6, 1973, as Related to Figures 8 and 9  
 (SKYLAB II Track is  $\sim 140^\circ$ , and antenna direction is  $\sim 240^\circ$ )

Time (GMT)			Wind Speed (knots)	Wind Direction (degrees)		
Hr	Min	Sec		Gradient Wind	Surface Wind	Relative to Antenna
$\theta \sim 45^\circ$						
18	56	2.3	12	060	030	150
18	56	17.6	15	070	040	160
18	56	32.8	18	070	040	160
18	56	48.1	20	070	040	160
18	57	3.3	26	080	050	170
18	57	18.6	30	090	060	180
18	57	33.8	33	120	090	210
18	57	49.1	36	130	100	220
18	58	4.3	36	150	120	240
18	58	19.6	33	160	130	250
18	58	34.8	30	180	150	270
18	58	50.1	25	190	160	280
18	59	5.3	20	200	170	290
18	59	20.6	18	210	180	300
18	59	35.8	17	210	180	300
18	59	51.1	15	210	180	300
19	00	6.3	13	270	190	310
19	00	21.6	11	210	180	300
$\theta \sim 30^\circ$						
18	56	5.8	10	070	040	160
18	56	21.0	14	080	050	170
18	56	36.3	17	080	050	170
18	56	51.5	19	090	060	180
18	57	6.8	22	100	070	190
18	57	22.0	25	110	080	200
18	57	37.3	27	120	090	210
18	57	52.5	29	130	100	220
18	58	7.8	28	140	110	230
18	58	23.0	26	160	130	250
18	58	38.7	23	170	140	260
18	58	53.5	20	180	150	270
18	59	8.8	18	170	160	280
18	59	24.5	17	210	180	300
18	59	39.7	15	210	180	300
18	59	54.5	14	210	180	300
19	00	10.2	13	210	180	300
19	00	25.0	11	200	170	290

(1) Surface wind direction = (gradient wind direction  $-30^\circ$ )

(2) Relative wind direction = (surface wind  $-240^\circ$ )

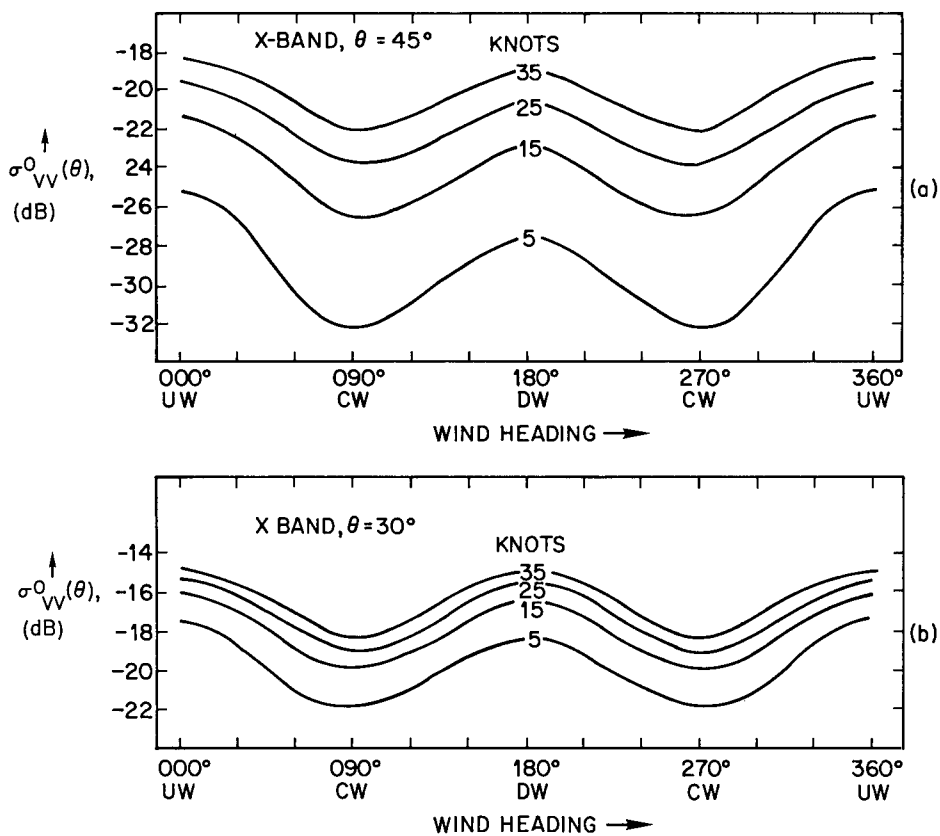


Fig. 8 — Variation of X-Band  $\sigma_{VV}^0(\theta)$  as a function of wind heading for four selected wind speeds (in knots) as interpolated from NRL empirical model.

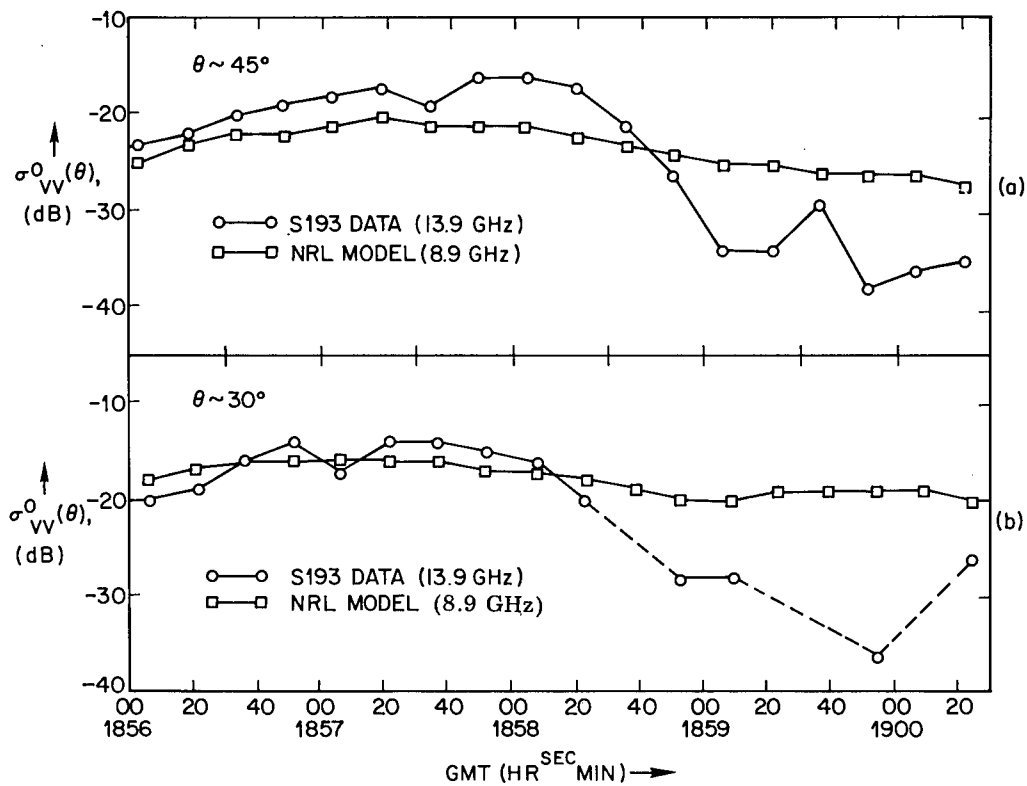


Fig. 9 — Comparison of  $\sigma_{VV}^0(\theta)$ , S193 data at 13.9 GHz as a function of time with interpolated NRL model data at 8.9 GHz (missing points are interpolated with dashed lines) for two incidence angles.

## CONCLUSIONS AND RECOMMENDATIONS

The data of the June 5, 1973, pass showed good agreement with both the NRL empirical and theoretical models within their domains of applicability. Since a practically uniform wind field was present over the Gulf of Mexico on that day, these conditions provided an ideal test case, and good agreement was to be expected.

The data of June 6, 1973, required more detailed analysis due to the rapidly varying wind speeds and directions around Hurricane AVA. If the speeds and the directional properties of the wind field are analyzed, then a reasonable comparison can be made with the interpolated NRL empirical model for the first half of the data points, which cover approximately the northeast quadrant of Hurricane AVA. Recent information [17] indicates that the disparity between the NRL empirical model and the second half of the data points (approximately the southeast quadrant of AVA) can probably be explained by attenuation in rain bands or by a forward pitch of the space craft, which caused significant changes in the doppler shift so that  $\sigma^{\circ}$  decreased. In any case, these later data points need to be carefully evaluated. Further scatterometer data analyses for hurricanes are recommended as a basis for quantitative estimates of variations in normalized cross section due to rainbands and spacecraft attitudes.

The results of the data analysis so far are encouraging; however, considerably more data (both satellite data and sea truth) need to be analyzed so that the scatterometer and its utilization can be adequately evaluated. The relationship between the measured radar cross section and the ocean wind and wave conditions is complex. Accordingly, before accurate oceanographic remote sensing can be achieved, many parameters, including wind speed, wind direction, barometric pressure, air and sea temperatures, wave height and slope distributions, and rain and cloud conditions, must be considered. Information about rain attenuation can be obtained from radiometric measurements and also from comparison of the polarized (HH and VV) and cross-polarized (HV and VH) scatterometer measurements. Statistical analyses of many scatterometer measurements (data from NRL and other laboratories) should be made in order to obtain correlations between ocean parameters and radar cross section measurements under varying conditions. In summary, it can be stated that the S193 scatterometer provides basic radar scattering data about the Earth's surface over which it passes; further detailed analyses based upon scatterometer measurements are recommended as a means to accurate interpretation of such data.

## ACKNOWLEDGMENTS

The authors gratefully acknowledge the contributions of Lyle Schroeder, NASA/Langley Research Center, and of John Daley and Denzil Stilwell, Naval Research Laboratory, who provided advice throughout the preparation of this report.

REFERENCES

1. J.R. Apel, Statement before the Subcommittee on Space Science and Applications, Committee on Science and Astronautics, House of Representatives, March 6, 1974.
2. C.T. Swift and L.T. Jones, Jr., "Satellite Radar Scatterometry," presented at the IEEE Intercon, session 34/4; March 26, 1974.
3. R.K. Moore *et al* "Simultaneous Active and Passive Microwave Response of the Earth — The SKYLAB Radsat Experiment," Proc. of 9th Symposium on Remote Sensing of the Environment, Ann Arbor, Mich., April 1974.
4. J.W. Wright, "A New Model for Sea Clutter," *IEEE Trans.*, Vol. AP-16, pp. 217-223, 1968.
5. G.R. Valenzuela, M.B. Laing, and J.C. Daley, "Ocean Spectra for the High-Frequency Waves as Determined from Airborne Radar Measurements," *J. Marine Research*, Vol. 29, pp. 69-84, May 1971.
6. N.W. Guinard and J.C. Daley, "An Experimental Study of a Sea Clutter Model," *Proc. IEEE*, Vol. 58, pp. 543-550, 1970.
7. G.R. Valenzuela, "Scattering of Electromagnetic Waves from a Tilted Slightly Rough Surface," *Radio Science*, Vol. 3, pp. 1057-1066, 1968.
8. J.C. Daley, W.T. Davis, and N.R. Mills, "Radar Sea Return in High Sea States," NRL Report 7142, Sept. 25, 1970.
9. J.C. Daley, "An Empirical Sea Clutter Model," NRL Memo Report 2668, Oct. 1973.
10. J. Hayes, *et al*, "A Preliminary Analysis of the Surface Truth Data to Be Correlated with the SKYLAB II Data Obtained for the S193 Investigators," University Institute of Oceanography, City University of New York, Aug. 1973.
11. SKYLAB II/Pass 5, ITNC R/S 5 3A-DPCA-4-5R5, S062-11, NASA/Johnson Space Center, Sept. 16, 1974. (This replaces Data S062-11; Dec. 30, 1973.)
12. SKYLAB II/Pass AVA, CTNC R/S 5 3A-DPCA-AVAR5, Note 2, S062-11, Sept. 7, 1974. (This replaces Data S062-11, Dec. 30, 1973.)
13. S193 Microwave Radiometer/Scatterometer/Altimeter, Flight Hardware Configuration Specification, Spec. No. SvS7846, Rev. C., April 27, 1972, Space Systems Organization, General Electric Co.
14. C.M. Cox and W.H. Munk, "Measurement of the Roughness of the Sea Surface from Photographs of the Sun's Glitter," *J. Opt. Soc. Am.*, Vol. 44, pp. 838-850, 1954.

15. D. Stilwell, Jr., and R.O. Pilon, "Directional Spectra of Surface Waves from Photographs," *J. Geophys. Res.*, Vol. 79, pp. 1277-1284, March 20, 1974.
16. F.A. Berry, Jr., E. Bollay, and N.R. Beers, eds., *Handbook of Meteorology*, McGraw-Hill Book Co., New York , pp. 860-861, 1945.
17. J.P. Claassen, Private communication.